

## Electron Microscopy of Gold-Containing $\text{Ag}_3\text{Sn}$ Splat-Cooled Ribbons\*

MANOHAR L. MALHOTRA

*School of Dentistry, University of Michigan,  
Ann Arbor, Michigan 48109*

---

Splat-cooled ribbons of gold-containing Ag-Sn alloys were prepared and studied primarily by electron optical methods. The microstructure revealed well-defined grains separated by sharp boundaries. Electron microprobe analysis confirmed that the ribbons are homogeneous, with gold distributed uniformly all over the surface. Selected area electron diffraction further proved that these ribbons belong to single phase  $\gamma$ , an  $\text{Ag}_3\text{Sn}$  compound.

---

### Introduction

During the last decade, rapid cooling from the melt to form splat-cooled ribbons has been shown to result in the formation of metastable phases in a number of metallic systems. Information on these systems is readily available in the literature. However, little has been done to investigate these ribbons using the modern techniques of electron microscopy. The gun technique produces rapidly solidified ribbons with certain thin areas suitable for direct examination by high-energy transmission electron microscopy.

In dentistry,  $\text{Ag}_3\text{Sn}$  alloy particles (74% Ag and 26% Sn) are reacted with mercury to produce an amalgam which is widely used as a restorative material. Recently, some attempts have been made to modify this basic  $\text{Ag}_3\text{Sn}$  alloy by replacing silver with different elements such as gold, copper, or manganese in an effort to produce an amalgam free of the  $\gamma_2$  ( $\text{Sn}_{7-8}\text{Hg}$ ) phase, an undesirable constituent in the amalgam [1-

---

\* This work was done at the Materials Science Department of the University of Virginia, Charlottesville, Virginia 22903. Presented in part at the 52nd general meeting of the International Association for Dental Research, Atlanta, Georgia, March, 1974.

11]. The present study is focused on the gold-containing Ag-Sn splat-cooled ribbons. Some microstructural details from these ribbons were reported previously [12] using primarily x-ray diffraction and scanning electron microscopy. The present work is intended to study the homogeneity of these ribbons using electron microprobe analysis and also to examine their structural features directly in the high-voltage transmission electron microscope. Grain orientations were analyzed using selected area electron diffraction patterns.

It is well known that splat-cooled ribbons of any material (metal or an alloy) have pores scattered all over the surface. In the gold-containing Ag-Sn splat-cooled ribbons, it is found that there are areas near the pores with varying thickness from  $\sim 20 \mu$  to  $< 1 \mu$ . These thin areas ( $\sim 1 \mu$ ) were observed directly in the high-voltage transmission electron microscope (RCA-500 kV) without further polishing, etching, or thinning of the splat-cooled ribbons.

## Theory

From the literature, the  $\gamma$  (Ag<sub>3</sub>Sn) phase has been found to have an orthorhombic unit cell [13, 14] with lattice parameters  $a_0 = 2.995$ ,  $b_0 = 5.159$ , and  $c_0 = 4.781$  Å. The standard equations of this system for  $d_{hkl}$ , the distance between the adjacent planes in the set ( $hkl$ ), and for angle  $\phi$ , the angle between the planes ( $h_1k_1l_1$ ) of spacing  $d_1$  and ( $h_2k_2l_2$ ) of spacing  $d_2$  were used in indexing the selected area electron diffraction patterns.

The average grain size was measured from the linear intercept length  $L$  obtained as

$$L = \frac{L_T}{MN}$$

where  $L_T$  equals the total test line length,  $N$  is the number of grain-boundary intersections, and  $M$  is the magnification used in the particular photomicrograph [15, 16].

## Experimental Procedures

Splat-cooled ribbons of gold-containing Ag-Sn alloys were prepared by the procedures outlined previously [12]. The ribbons were etched in a 30% nitric acid solution until the structure was developed for metallographic examination in the SEM. An Ortec Si (Li) x-ray energy-dispersive spectrometer was attached to the SEM in order to obtain x-ray emission spectra of elements present at any point on the specimen

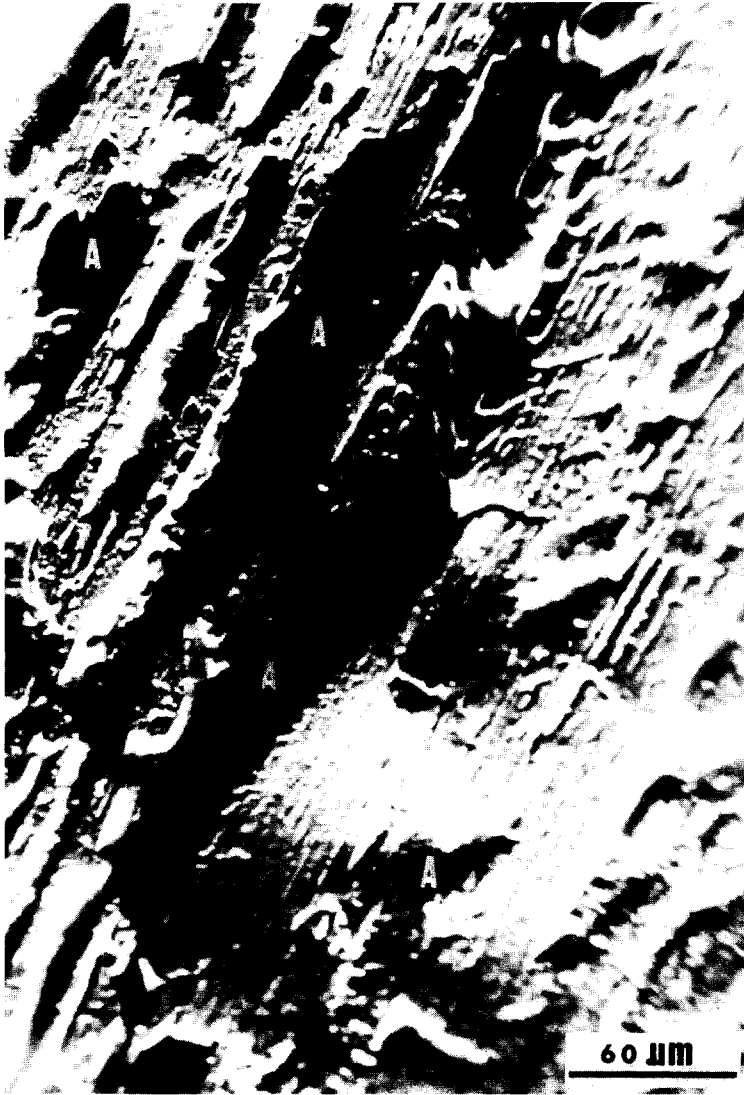


FIG. 1. Typical scanning electron photomicrograph of a splat-cooled Ag-Sn-Au alloy ribbon (59% Ag, 26% Sn, and 15% Au) surface. Areas marked A show pores scattered all over the ribbon surface.



FIG. 2. (a) Typical scanning electron photomicrograph of a splat-cooled Ag-Sn-Au alloy ribbon (59% Ag, 26% Sn, and 15% Au) surface after it is etched in a 30% nitric acid solution.

Microstructure reveals grains separated by sharp boundaries.

surface. Overlapping of the x-ray spectra obtained from various places on the specimen surface confirmed the homogeneity of these splat-cooled ribbons. The ribbons were examined in the high-voltage transmission electron microscope (RCA-500 kV) operated at 400 kV. The selected area electron diffraction patterns obtained from different grains identified their orientations. Average grain size in these splat-cooled ribbons was determined from a relation as described in the previous section.

## Results and Discussion

Figure 1 shows a typical scanning electron photomicrograph of a 15% gold-containing Ag-Sn splat-cooled alloy ribbon (59% Ag, 26% Sn, and 15% Au), as prepared. It shows pores (areas marked A) scattered all over the surface. Near the pores, there are regions  $\sim 1 \mu$  thick which are studied directly in the high-voltage transmission electron microscope.

Figure 2(a) shows a scanning electron photomicrograph of a splat-

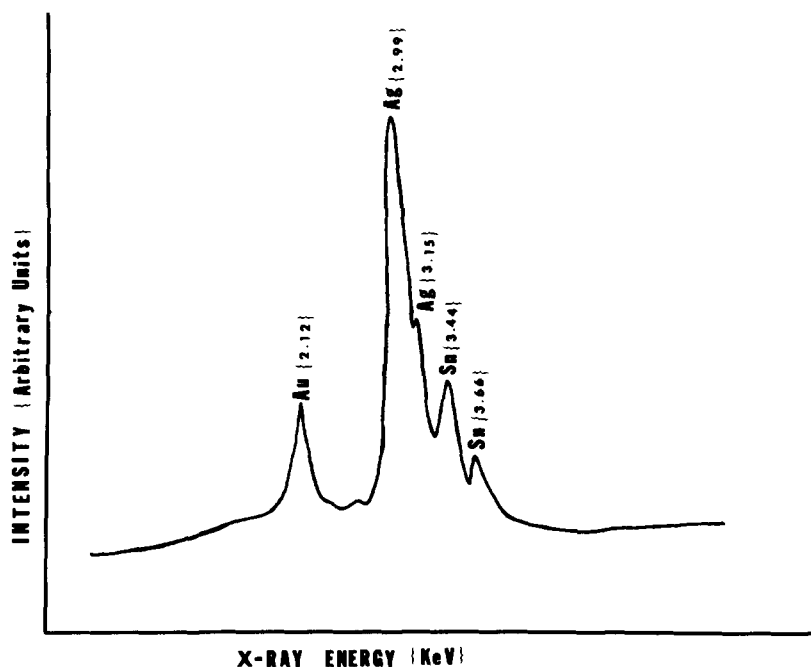


FIG. 2. (b) X-ray emission spectrum obtained from the photomicrograph shown in (a). Overlapping of the spectra obtained from the different regions confirmed the homogeneity of the alloy ribbons. This implies that gold is distributed uniformly all over the Ag-Sn phase grains.

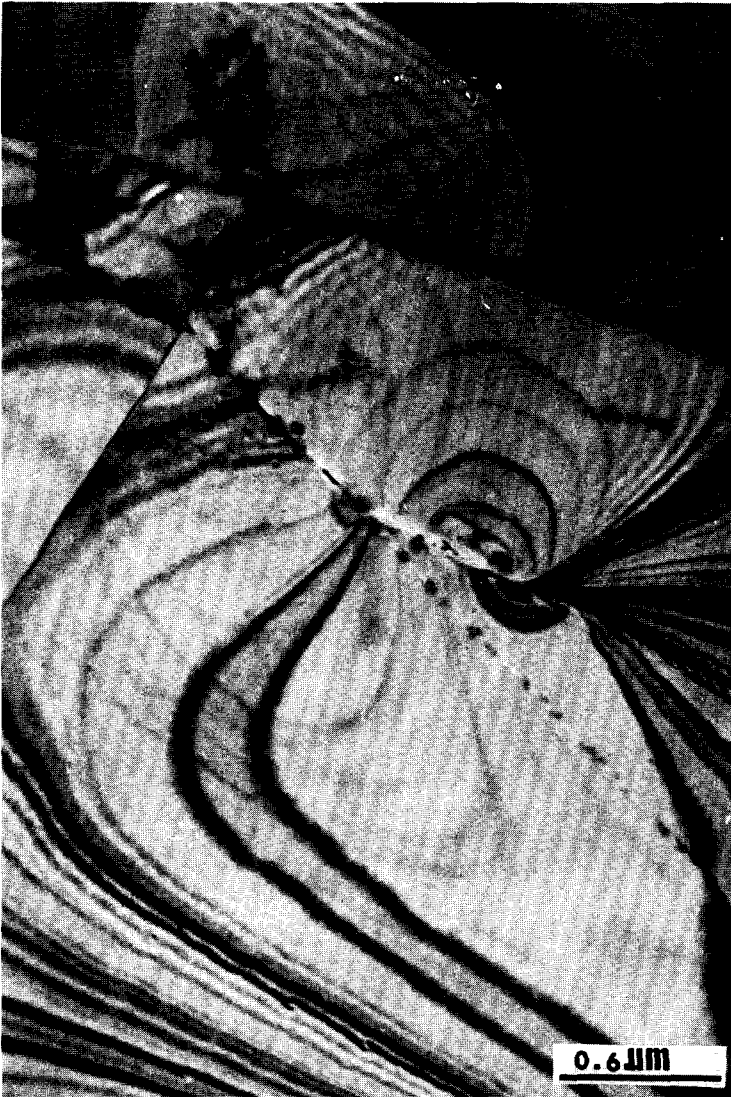
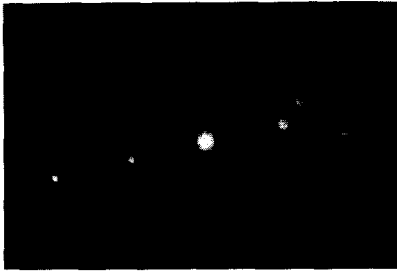
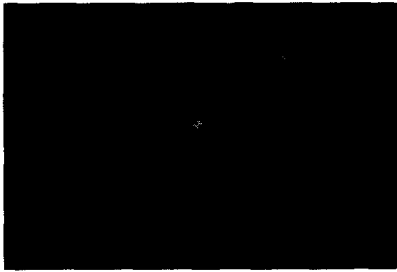
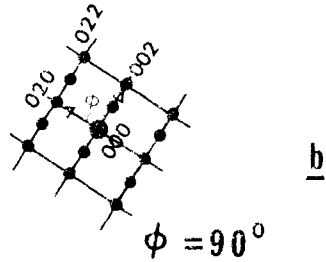


FIG. 3. (a) Transmission electron photomicrograph of a splat-cooled Ag-Sn alloy ribbon (74% Ag and 26% Sn), showing grains separated by sharp boundaries. The bend contours owing to the buckling of the specimen are clearly observed.



(100) Reflection



(131) Reflection

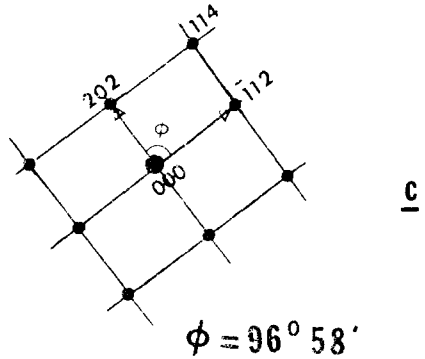


FIG. 3. (b) and (c) Typical selected area electron diffraction patterns were obtained from the photomicrograph shown in (a). The diffraction patterns correspond to  $\gamma$  ( $\text{Ag}_3\text{Sn}$ ) phase. Extra spots in (b) show superlattice reflections, commonly observed in  $\text{Ag}_3\text{Sn}$ .

cooled ribbon surface of the same alloy composition. The surface was etched in a 30% nitric acid solution for several minutes ( $\sim 5$  min) until the structure is developed for metallographic examination. In the photomicrograph the areas marked A show grains separated from each other by well-defined boundaries. Electron microprobe analysis of these areas A [Fig. 2(a)] is shown in Fig. 2(b). The observed x-ray emission spectrum shows the presence of Ag, Sn, and Au with uniform intensity of these elements over the entire surface. This proves the following results: (1) The ribbons are homogeneous. Also, gold is distributed uniformly within the Ag-Sn grains. (2) The addition of gold up to 15%



FIG. 4. (a) Transmission electron photomicrograph of a gold-containing Ag-Sn alloy ribbon (65% Ag, 26% Sn, and 9% Au), showing grains separated from each other by sharp boundaries.



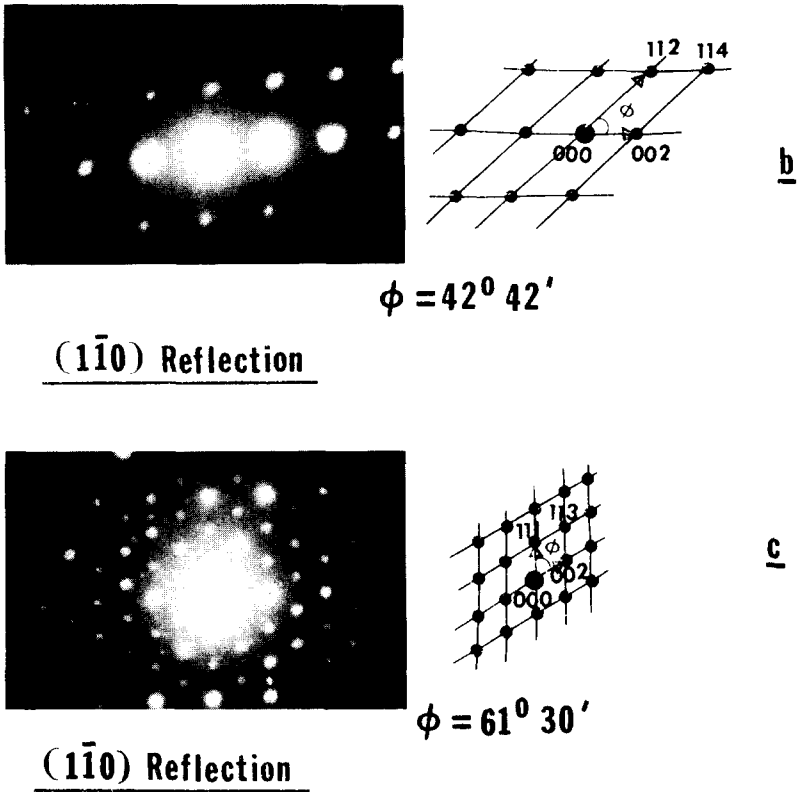


FIG. 4. (b) and (c) Typical selected area electron diffraction patterns were obtained from the photomicrograph shown in (a). The diffraction patterns correspond to  $\gamma$  ( $\text{Ag}_3\text{Sn}$ ) phase.

did not show the formation of any new phase in the gold-containing Ag-Sn alloy ribbons.

Figures 3-5 show transmission electron photomicrographs and their corresponding selected area electron diffraction patterns for Ag-Sn splat-cooled ribbons containing 0, 9, and 15% gold. The studies were made on a high-voltage transmission electron microscope operated at 400 kV. The microstructure was found to contain well-defined grains separated from each other by sharp boundaries. Figure 3(a) shows a transmission electron photomicrograph of an alloy ribbon surface containing silver and tin (74% Ag and 26% Sn). The sharp grain boundaries of Ag-Sn particles are clearly visible along with the bend contours present owing to the buckling of the specimen. Figures 3(b) and 3(c)



FIG. 5. (a) Transmission electron photomicrograph of a high content gold-containing Ag-Sn splat-cooled alloy ribbon (59% Ag, 26% Sn, and 15% Au), showing grains separated from each other by sharp boundaries.

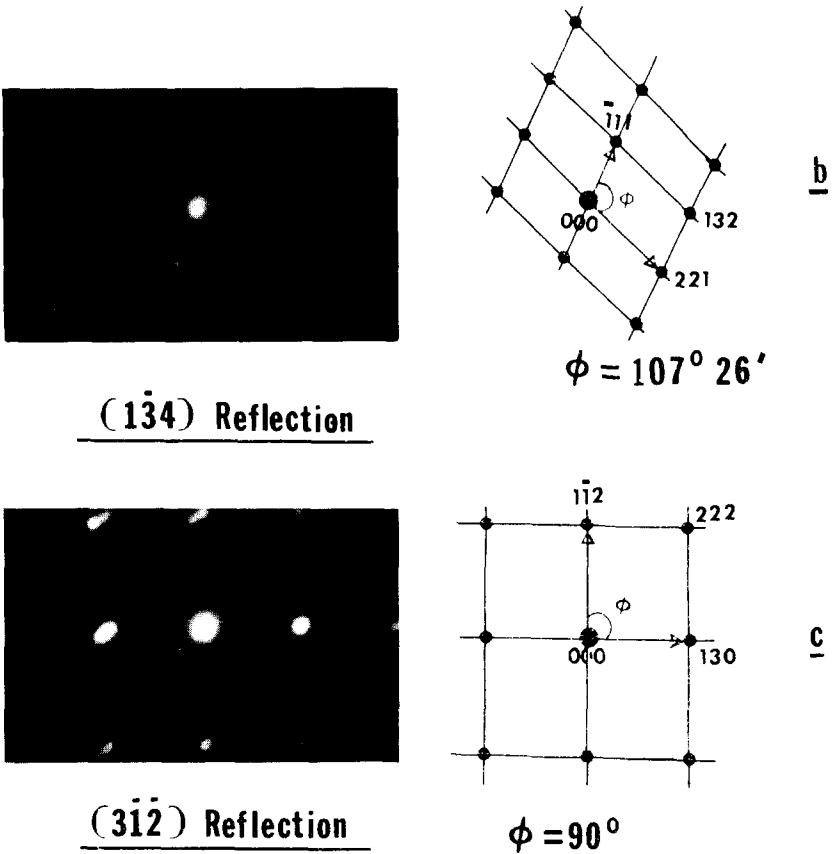


FIG. 5. (b) and (c) Typical selected area electron diffraction patterns were obtained from the photomicrograph shown in (a). The broad reciprocal lattice points as seen in (c) are typically observed in platelet specimens. The diffraction patterns correspond to  $\gamma$  ( $\text{Ag}_3\text{Sn}$ ) phase.

show typical selected area electron diffraction patterns obtained from the photomicrograph shown in Fig. 3(a). The analysis showed that these diffraction patterns correspond to  $\gamma$  ( $\text{Ag}_3\text{Sn}$ ) phase, as expected. In Fig. 3(b) there are extra diffraction spots along the  $c$  direction corresponding to superlattice reflections, commonly reported in  $\text{Ag}_3\text{Sn}$ . Figure 4(a) shows a transmission electron photomicrograph of a gold-containing  $\text{Ag-Sn}$  alloy ribbon surface (65% Ag, 26% Sn, and 9% Au). The grains have been clearly identified as having sharp boundaries. Some grains show a fine precipitate which may correspond to either a new phase or a fine

structure within the grains. So far, the observed selected area electron diffraction patterns, some of which are shown in Figs. 4(b) and 4(c), showed reflections only from  $\gamma$  ( $\text{Ag}_3\text{Sn}$ ) phase. Figure 5(a) shows a transmission electron photomicrograph of a high-content gold-containing Ag-Sn alloy ribbon (59% Ag, 26% Sn, and 15% Au). As observed in the Ag-Sn alloy ribbons, the microstructure in this case also consists of grains separated from each other by sharp boundaries. The microstructure is extremely fine-grained when the gold content is above the limit of metastable solid solubility. A large amount of substructure was possibly formed during the solidification of individual grains, leading to the granular structure. Selected area electron diffraction patterns shown in Figs. 5(b) and 5(c) show reflections only from  $\gamma$  ( $\text{Ag}_3\text{Sn}$ ) phase. In Fig. 5(c), the reciprocal lattice points are broadened as typically observed in thin platelet specimens. Reflections from any other phase, if at all present, have not been yet detected.

X-ray diffraction results as reported earlier [12] showed only  $\gamma$  ( $\text{Ag}_3\text{Sn}$ ) phase in the gold-containing Ag-Sn splat-cooled ribbons. However, there was a consistent reduction in lattice parameters of the gold-containing  $\text{Ag}_3\text{Sn}$  ribbons when compared to the pure  $\text{Ag}_3\text{Sn}$  splat-cooled ribbons. This change in lattice parameters would hardly be detected in the present study of electron diffraction patterns. King [17] has also reported that gold substitutionally added in amounts greater than 30% in the  $\text{Ag}_3\text{Sn}$  lattice results in a contraction of lattice; the contraction was insignificant in the present range of gold concentrations added to  $\text{Ag}_3\text{Sn}$ . The splat-cooling process might also be responsible, in part, to force gold in the  $\text{Ag}_3\text{Sn}$  lattice structure. This further avoids the formation of any other new phase.

Average grain size as measured from several scanning electron photomicrographs is  $3.2 \mu$ . An average grain size of  $2.0 \mu$  was obtained from several transmission electron photomicrographs taken only near the pores of the ribbons. This grain size corresponds only to localized areas and does not represent the average grain size of the bulk material. However, it is believed that the average grain size of  $3.2 \mu$  as obtained from several scanning electron photomicrographs relates closely to the grain size of the bulk material.

## Summary

Microstructure from properly etched splat-cooled ribbons revealed large grains ( $3.2 \mu$  average size) separated from each other by sharp boundaries. Electron microprobe analysis has confirmed that the gold-

containing Ag-Sn ribbons are homogeneous. Gold is distributed uniformly all over the ribbon surface. The high-voltage transmission electron microscope (RCA-500 kV) has also revealed microstructure from the localized thin areas in the ribbons as prepared without any polishing, etching, or thinning of the specimens. The microstructure as revealed by transmission electron microscopy showed small grains ( $2.0 \mu$  average size) separated from each other by sharp boundaries. Selected area electron diffraction also proved that these ribbons correspond to single phase  $\gamma$ , an  $\text{Ag}_3\text{Sn}$  compound.

*The author is grateful to Professor Kenneth R. Lawless for his keen interest throughout the investigation. Financial support of the National Institute of Dental Research, National Institutes of Health, under Research Grant No. DE-02111, Bethesda, Maryland 20014 is acknowledged.*

## References

1. L. B. Johnson, A new dental alloy. IADR Meeting (DMG Microfilm), Chicago, Illinois (1971).
2. Manohar L. Malhotra, Microstructure of dental alloys and amalgams, Ph.D. Dissertation, University of Virginia (May, 1974).
3. D. B. K. Innes and W. V. Youdelis, Dispersion strengthened amalgams, *Can. Dent. Assoc. J.* **29**, 587-593 (1963).
4. R. M. Waterstrat, N. W. Rupp, and R. C. Manuszewski, Improved creep behavior and removal of gamma-2 phase in dental amalgams containing manganese, IADR Meeting (DMG Microfilm), Miami Beach, Florida (March, 1976).
5. C. E. Guthrow, L. B. Johnson, and K. R. Lawless, Corrosion of dental amalgam and its component parts, *J. Dent. Res.* **46**, 1372-1381 (1967).
6. K. D. Jørgensen and Tsuyoshi Saito, Structure and corrosion of dental amalgams, *Acta Odont. Scand.* **28**, 129-142 (1970).
7. R. S. Mateer and C. D. Reitz, Corrosion of amalgam restorations, *J. Dent. Res.* **49**, 399-407 (1970).
8. D. E. Grenoble and J. L. Katz, Pressure-induced disappearance of the  $\gamma_2$  ( $\text{Hg Sn}_{7-8}$ ) phase in dental amalgam, *J. Dent. Res.* **50**, 109-115 (1971).
9. Gene A. Holland and Kamal Asgar, Some effects in the phases of amalgam induced by corrosion, *J. Dent. Res.* **53**, 1245-1254 (1974).
10. N. K. Sarkar, G. W. Marshall, J. B. Moser, and E. H. Greener, In vivo and in vitro corrosion products of dental amalgam, *J. Dent. Res.* **54**, 1031-1038 (1975).
11. Manohar L. Malhotra and Kamal Asgar, Relationship between microstructure, creep, and strength in dental amalgam, IADR Meeting (DMG Microfilm), Miami Beach, Florida (March, 1976).
12. Manohar L. Malhotra and Kunal Basu, Microstructure in gold-containing  $\text{Ag}_3\text{Sn}$  splat-cooled ribbons, *Metallography* **8**, 515-523 (1975).
13. O. Nial, A. Almin, and A. Westgren, Röntgenanalyse der Systeme Gold-Antimon und Silber-Zinn, *Z. Physik. Chemie* **B14**, 81-90 (1931).

14. M. Hansen, *Constitution of Binary Alloys*, McGraw-Hill, New York (1958).
15. R. T. Dehoff and F. N. Rhine, *Quantitative Microscopy*, McGraw-Hill, New York (1968).
16. Ervin Underwood, *Metals Handbook, 8th Edition*, Vol. 8, American Society for Metals, Metals Park (1973), p. 37.
17. H. W. King, Quantitative size-factors for metallic solid solutions, *J. Mater. Sci.* **1**, 79–90 (1966).

*Received May 17, 1976*